

# Effect of crystallographic anisotropy on the nature of the instability of a rounded crystal

D. E. Ovsienko, A. M. Ovrutskii, and O. P. Fedorov

*Institute of Metal Physics, Academy of Sciences of the Ukrainian SSR*

(Submitted 11 January 1991; resubmitted 22 April 1991)

Zh. Eksp. Teor. Fiz. **100**, 939–947 (September 1991)

The instability of a rounded crystal has been studied by direct observation and numerical simulation. Distortions of the rounded shape along the predominant  $\langle 100 \rangle$  directions arise in the stage of growth in the kinetic regime, i.e., under conditions such that the growth pattern is controlled exclusively by surface processes. Depending on the lattice structure (bcc or fcc), either (a) only the predominant  $\langle 100 \rangle$  protuberances form or (b) both the predominant protuberances and additional  $\langle 111 \rangle$  protuberances form. The numerical simulation of the process shows that the differences in the morphology of the protuberances are determined by the magnitude of the anisotropy, not by its angular distribution. Protuberances appear or are suppressed upon small changes in the anisotropy parameter. The effects depend on the magnitude of the kinetic coefficient and on the initial supercooling of the melt.

## INTRODUCTION

The shape of a crystal grown from the melt is known to depend strongly on the anisotropy of the surface energy  $\sigma$ . In particular, the fraction of the equilibrium shape made up of a given face is smaller, the higher the indices of this face.<sup>1</sup> Cubic crystals of substances having a low melting entropy ( $Q/kT_0 < 2$ , where  $Q$  is the latent heat of melting, and  $T_0$  is the melting point) have an atomically rough crystal-melt interface, with a slight anisotropy of  $\sigma$  (Refs. 2 and 3). In this case the crystals are rounded in shape, without any evidence of plane faces or macroscopic steps. This shape is evidence of an isotropic growth of the crystals. These morphological features, along with the linear dependence of the growth velocity  $V$  on the supercooling of the melt,  $\Delta T$ , i.e.,  $V = B\Delta T$  ( $B$  is a kinetic coefficient), are characteristic features of normal (continuous) crystal growth.<sup>3,4</sup> A detailed study of the growth of a rounded crystal at a small value of  $\Delta T$  has revealed a slight anisotropy of the velocity.<sup>5</sup> The subsequent formation of dendrites from an initially rounded crystal is predetermined by some a certain crystallographic direction ( $\langle 100 \rangle$  in the case of fcc and bcc crystals). As was shown in Ref. 6, such dendrites can undergo a steady-state growth by virtue of the anisotropy of the surface energy  $\sigma$  (or of the kinetic coefficient  $B$ ). All these results indicate that a small anisotropy of  $\sigma$  (or of  $B$ ) plays a fundamental role in determining the shape of crystals which grow by the normal mechanism.

The formation of protuberances on an initially rounded crystal results from both anisotropic processes at the interface and isotropic heat-transfer (or mass-transfer) processes in the melt. This stage of the growth is definitely nonsteady, so it is difficult to study by analytic methods. Our purpose in the present study was to learn about the initial stage of the formation of protuberances on a macroscopically rounded crystal through experiments and numerical simulation. Calculations of this sort have been carried out previously for tin crystals.<sup>7</sup> In the present study the calculations were extended to transparent organic substances, whose crystal growth can be observed directly.

## EXPERIMENTAL RESULTS AND DISCUSSION

Table I shows the properties of the four substances studied. We see that all have low melting entropies ( $Q/kT < 2$ )

and differ in pairs in the type of crystal lattice. In addition, cyclohexanol has an anomalously low kinetic coefficient  $B$ . It has been shown previously<sup>5</sup> that at small values of  $\Delta T$  ( $\sim 0.1$  K) the crystals of these substances are rounded. When they reach a certain size, protuberances form on them. Six main  $\langle 100 \rangle$  protuberances form on the crystals with an fcc lattice (cyclohexane and cyclohexanol; four protuberances lying in the plane of observation are visible in Fig. 1). Six main  $\langle 100 \rangle$  protuberances and eight additional  $\langle 111 \rangle$  protuberances form in the succinonitrile and camphene crystals. The latter protuberances grow more slowly, and they are later suppressed by  $\langle 100 \rangle$  branches as the growth continues. Under certain conditions, dendrites can also form from  $\langle 111 \rangle$  protuberances. As was shown in Ref. 8, the morphological features of these dendrites are determined to a large extent by the growth in a nonpreferred direction. It has also been established that only the  $\langle 100 \rangle$  principal protuberances arise on a rounded succinonitrile crystal when the initial supercooling of the melt is increased to 0.5 K.

The experimental kinetic coefficients found for organic crystals in Ref. 9 can be used to calculate the radii of relative and absolute stability of the rounded growth forms, i.e.,  $R_s$  and  $R_a$ . The radius  $R_s$  is the crystal radius at which a protuberance which has arisen on the surface of the crystal grows no more rapidly than the rest of the surface. This radius corresponds to a smoothing of a distortion which has arisen.<sup>10</sup> Figure 2 shows theoretical results on  $R(\Delta T)$  calculated from Eqs. (1) for  $l = 3$ , using the parameters given in Table I:

$$R_a = \frac{1}{2}R_{cr} [1 + \frac{1}{2}(l+2)(1+\kappa l)] \times \left\{ 1 + \left[ 1 + 2\alpha_1 \frac{(l+2)(1+\kappa l)}{[1 + \frac{1}{2}(l+2)(1+\kappa l)]^2} \right]^{\frac{1}{2}} \right\},$$

$$R_s = \frac{1}{2}R_{cr} \left[ 1 + \frac{1+\kappa l}{l-2} (L + \alpha_1) \right] \times \left\{ 1 + \left[ 1 + 4\alpha_1 \frac{(1+\kappa l)(l-2)(L-1)}{[(l-2) + (1+\kappa l)(L + \alpha_1)]^2} \right]^{\frac{1}{2}} \right\},$$

where

$$R_{cr} = \frac{2T_0\Gamma}{T_0 - T_\infty}, \quad L = \frac{1}{2}(l-1)(l+2), \quad \alpha_1 = \frac{K_m}{QBR_{cr}},$$

TABLE I.

Substance	$Q/kT_0$	Lattice type	Crystal-melt surf. energy, $J/m^2$	Thermal conductivity of melt, $\alpha$ , $cm^2/s$	Experimental instability radius, $\mu m$	Kinetic coefficient, $cm/(s \cdot K)$
Succinonitrile	1,35	bcc	$\sim 9 \cdot 10^{-3}$	$1,16 \cdot 10^{-3}$	300 ( $\Delta T = 0,1 K$ )	17—50
Cyclohexane	1,15	fcc		$7,8 \cdot 10^{-4}$	400 ( $\Delta T = 0,15 K$ )	30—150
Cyclohexanol	0,7	fcc	$9,3 \cdot 10^{-3}$	$1,35 \cdot 10^{-2}$	300 ( $\Delta T = 0,1 K$ )	$1,6 \cdot 10^{-2}$
Camphene	1,15	bcc		$\sim 1 \cdot 10^{-3}$	300 ( $\Delta T = 0,1 K$ )	$>1$

$K_m$  is the thermal conductivity of the melt,  $K_{cr}$  is that of the crystal,  $\kappa = 1 + K_{cr}/K_m$ , and  $\Gamma = \sigma/Q$ .

The curves for succinonitrile (Fig 2a) and cyclohexane (Fig. 2b) essentially coincide. Also shown here is the  $\Delta T$  dependence of the characteristic diffusion radius  $R_d = \alpha/(Q/C)B$ , where  $\alpha$  is the thermal diffusivity of the melt and  $C$  is its specific heat. For  $R < R_d$ , the crystal growth is controlled exclusively by processes at the boundary. When the opposite inequality holds, the growth is controlled by heat transfer in the interior of the melt. A comparison of these calculated results with experimental data shows that the succinonitrile crystals visible under a microscope grow deep in the diffusion regime, while cyclohexanol crystals spend a long part of their growth time in the kinetic regime. This difference is a consequence of the large difference in kinetic coefficients.

During the stage of growth in the kinetic regime for the cyclohexanol crystals, an anisotropy of the velocity has been

found. This anisotropy causes a slight distortion of the rounded crystal in the four  $\langle 100 \rangle$  directions in the observation plane. When the value  $R = R_s$  is reached, distortions with a curvature different from that of the original crystal appear on the surface of the crystal. These distortions subsequently develop into dendrites. For cyclohexane, which has the same crystal lattice, precisely the same protuberances form, but in this case the observed growth of the rounded crystal occurs deep in the diffusion regime, as in the case of succinonitrile (Fig. 2a). On the other hand, succinonitrile, with a bcc lattice, is characterized by the formation of eight additional  $\langle 111 \rangle$  protuberances in the initial stage of the instability of the rounded shape of the crystal. The same morphological feature is a property of the bcc camphene crystals.

These results can be used to refine our understanding of the nature of the instability of a rounded crystal. In the stage of growth in the kinetic regime, i.e., while the shape of the

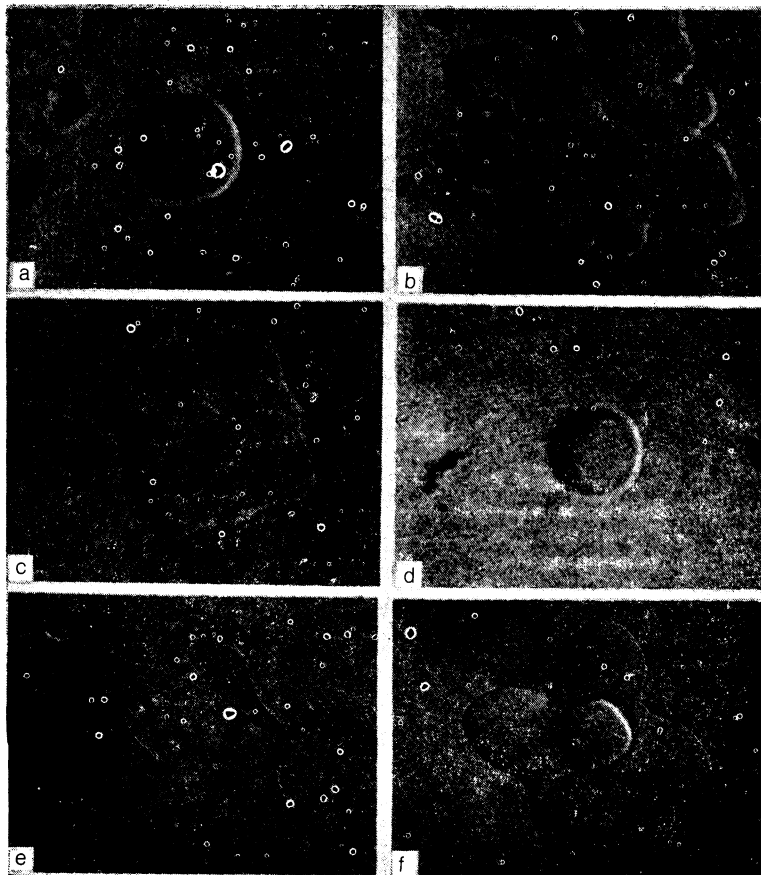


FIG. 1. Successive shapes of growing crystals associated with supercooling of a melt.  $\Delta T = 0.1 K$ . a-c—Succinonitrile; d-f—cyclohexanol.

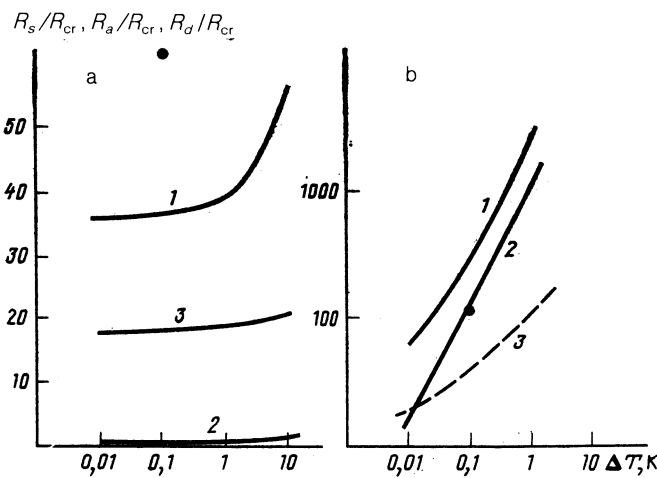


FIG. 2. The relative-stability radius  $R_s$  (1), the absolute-stability radius  $R_a$  (3), and the characteristic diffusion radius  $R_d$  (2), all divided by  $R_{cr}$ , as functions of the supercooling of the melt. a—Succinonitrile; b—cyclohexanol.

crystal is determined exclusively by processes at the interface, the rounded shape becomes distorted. In other words, even before the critical size is reached, protuberances are present on the crystal as a result of an anisotropy of surface processes. For this reason, there could hardly be any justification for invoking the concept of an absolute-stability radius  $R_a$ . In the diffusion growth regime, at  $R \gtrsim R_s$ , these protuberances develop along the  $\langle 100 \rangle$  direction in the case of a cubic lattice. The amplitude of the distortions which arise is determined by the nature of the anisotropy, by the absolute values of  $B$  and  $\sigma$ , and by the thermal properties of the melt. This amplitude imposes a certain morphology on the protuberances. Unfortunately, the specific way in which  $B$  and  $\sigma$  depend on the crystallographic direction is not known. In particular, the difference between this dependence for the bcc lattice and that for the fcc lattice is not known. The subsequent analysis was carried out numerically. It was assumed that the nature of the anisotropy of  $B$  and  $\sigma$  is unknown; only the magnitude of this anisotropy was varied.

#### FORMULATION OF THE PROBLEM FOR THE NUMERICAL SIMULATION

Most previous numerical simulations of the evolution of the shape of crystals have dealt with the Laplace equation instead of the diffusion equation or the heat-conduction equation.<sup>6,11,12</sup> That approach is legitimate for the diffusion growth regime, in which the surface temperature or the concentration varies only slightly during the growth, since these properties are close to their equilibrium values. For supercooling of the melt corresponding to the experimental conditions discussed above, the size of a critical nucleating region is less than  $R_a$ , and in the course of the growth there is a transition from a kinetic regime to a diffusion regime. Under these conditions, it would be preferable to deal with the heat-conduction equation in the numerical simulation rather than to find solutions of the Laplace equation.

Experimental observations of crystals which are small in comparison with the cell dimensions fall in the category of a free three-dimensional growth. The growth of three-dimensional crystals has been simulated previously in several

studies (e.g., Refs. 13 and 14). Such calculations, however, require a lot of computer time. Most of the work on the simulation of dendrite growth has dealt with the two-dimensional case (a plane cell).

It is believed that growth in a plane cell and that in a three-dimensional cell are sufficiently alike that the mechanism for the shaping of the crystals can be determined. It was shown in Refs. 7 and 10 that the radii of absolute and relative stability are comparable in order of magnitude in the cases of two-dimensional and three-dimensional growth. According to Ref. 10, these radii are given by (1) for the case of two-dimensional growth in the diffusion regime. Expressions for  $R_a$  and  $R_s$  which incorporate the kinetics of surface processes are given in Ref. 7. The results calculated from expressions (1) agree with the results calculated from the expressions in Ref. 7 in the case of the growth of succinonitrile crystals, because of the large value of the kinetic coefficient  $B$  (the thermal conductivity in the solid phase was ignored). Substituting in numerical values of the properties of the succinonitrile crystals ( $Q/C = 23.12$  K,  $\Delta T = 0.2$  K), we find the following values for the relative-stability radius (expressed in units of the critical size of the crystal): 72.4, 89.4, 119.2, 156.4, and 250.3 for  $l = 3, 4, 5, 6,$  and  $8$ , respectively.

The method developed in Refs. 7 and 14 was used for the numerical solution of the problem. When the heat-conduction equation in polar coordinates is written in finite differences, the corresponding derivatives are expressed in terms of the temperature values at the nodes of an adjustable mesh based on radial lines. The lines of the mesh which intersect these radial lines are not circles, however. Those closest to the crystal reproduce the surface profile of the crystal, while those farthest from the crystal have the configuration of the edge of the cell (a circle).

The heat-balance condition at the interface is taken into account:

$$VQ = K_m \left( \frac{\partial T}{\partial n} \right)_m - K_{cr} \left( \frac{\partial T}{\partial n} \right)_{cr}, \quad (2)$$

where  $V$  is the local growth velocity (in the direction normal to the surface), and  $(\partial T / \partial n)_m$  and  $(\partial T / \partial n)_{cr}$  are the temperature gradients in the direction normal to the surface in the two phases. Since one of the node lines coincides with the surface of the crystal, the Gibbs-Thomson correction to the surface supercooling, as generalized by Herring<sup>15</sup> to the case of an anisotropic surface energy, can be taken into account in the calculation of the crystal growth velocity:

$$V = B(\varphi) [\theta_{sup} - \Gamma(\varphi) \bar{K}], \quad (3)$$

where  $\theta_{sup} = (T_0 - T_{srf}) / (T_0 - T_\infty)$  is the reduced supercooling at the given point on the surface,

$$\Gamma(\varphi) = (\Omega/kT) \left( \sigma + \frac{\partial^2 \sigma}{\partial \varphi^2} \right) = \Gamma_0 \left[ 1 + \frac{1}{\sigma} \frac{\partial^2 \sigma}{\partial \varphi^2} \right],$$

$\sigma$  is the surface-tension coefficient,  $\Omega$  is the volume of a molecule,  $K$  is the surface curvature,  $T_{srf}$  is the surface temperature, and  $T_\infty$  is the temperature far from the interface. The anisotropy of the growth velocity and that of the surface tension are specified by the functions

$$\sigma = \sigma_0 (1 + Z_1 \cos n\varphi), \quad B = B_0 (1 + Z_2 \cos n\varphi), \quad (4)$$

where  $\varphi$  is the angle between the normal to the given region

of the surface and the direction of the most rapid growth. In the case at hand we have  $n=4$  and  $\Gamma(\varphi) = \Gamma_0(1 - 15Z_1 \cos 4\varphi)$ , where  $\Gamma_0 = \sigma_0 \Omega / kT$  is the capillary length, and  $Z_1 < 1/15$ . We used the following parameter values:  $B = 50 \text{ cm}/(\text{s} \cdot \text{K})$ ,  $\alpha = 1.16 \cdot 10^{-3} \text{ cm}^2/\text{s}$ ,  $\Gamma_0 = 2 \cdot 10^{-8} \text{ cm}$ ,  $K_m = 5.32 \cdot 10^{-4} \text{ cal}/(\text{cm} \cdot \text{s} \cdot \text{K})$ , and various values of the factors  $Z_1$  and  $Z_2$ .

Preliminary calculations revealed that a large value of the kinetic coefficient imposes an additional restriction, namely a minimum time step, if the calculation is to converge. The thermal conductivity in the solid phase was ignored in order to reduce the computation time, and the last term in (2) was ignored.

Nonuniform meshes were used, with a step increasing along the radial lines with distance from the crystal. The initial size of the cell was chosen so that it was 40 times larger than the size of the crystal. The initial size of the cell was progressively increased in order to maintain this relation. Corrections were made for the position of the mesh nodes. The temperatures at the new nodes were found by interpolation. In the calculations on the case of a diffusion-limited growth, with  $B = \infty$ , the surface temperatures were set equal to their equilibrium values for the corresponding surface curvature:  $\theta_{\text{surf}} = \Gamma(\varphi) \tilde{K}$ . In addition, the growth velocity was found from condition (3).

### RESULTS OF THE NUMERICAL SIMULATION AND DISCUSSION

The numerical solutions give a complete description of the evolution of the shape of the crystal as well as information on the temperature field throughout the cell. Figure 3 shows successive profiles of crystals calculated for a relatively slight anisotropy of the surface energy and of the growth velocity. The rounded crystal with a size of  $15R_{\text{cr}}$  specified in the initial conditions had no protuberances (profile 1). As the growth proceeded, four protuberances developed along the directions of maximum growth velocity and of maximum surface energy, by virtue of the anisotropy of  $\sigma$  and  $B$ . As can be seen from profile 3 in Fig. 3, at a crystal size  $\sim 300R_{\text{cr}}$  some secondary protuberances are also quite evident (there are four additional protuberances; half of the crystal is shown in Fig. 3). These secondary protuberances grow in the direction of minimum  $B$  and  $\sigma$ . This crystal size is comparable to the corresponding experimental size. In the subsequent stages of the growth, the velocities of the principal and secondary protuberances are comparable in magnitude.

An increase in the anisotropy of the surface energy has the consequence that the secondary protuberances which arise when the crystal has reached a certain size grow more rapidly than the principal protuberances (Fig. 4). Analysis of the calculated isotherms [lines of constant relative super-

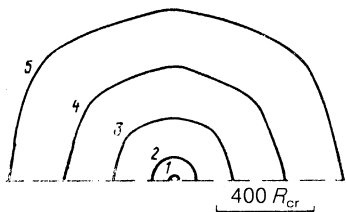


FIG. 3. Successive profiles of crystals for  $\Delta T = 0.2 \text{ K}$ ,  $Z_1 = 0.03$ , and  $Z_2 = 0.06$ . 1—Time interval  $t = 0.07 \text{ s}$ ; 2—0.13; 3—1.1; 4—3.6; 5—8.9 s.

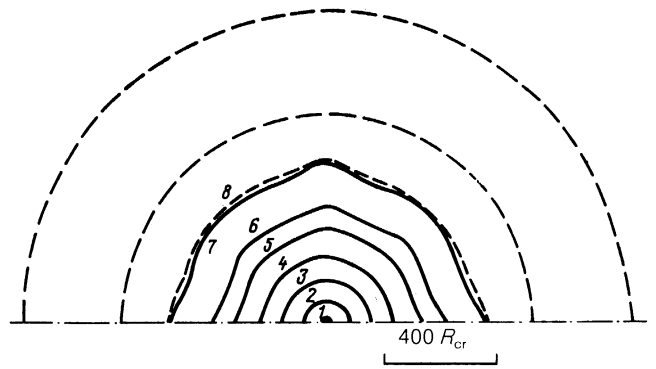


FIG. 4. Successive profiles of crystals and the temperature field for the last shape ( $\Delta T = 0.2 \text{ K}$ ,  $Z_1 = 0.05$ ,  $Z_2 = 0.06$ ).  $t = 0, 0.13, 0.47, 1.2, 2.4, 3.8, 7.5 \text{ s}$ .

cooling  $\Delta T_{\text{rel}} = (T_0 - T)/(T_0 - T_\infty)$  shows that the value of  $\Delta T_{\text{rel}}$  is larger near the secondary protuberances than near the principal ones. On the contrary, the considerable enhancement of the anisotropy of the kinetic coefficient (Figs. 5a,b) is responsible for the growth without secondary protuberances. That the appearance of the additional protuberances is associated with the size of the kinetic coefficient follows from Fig. 6, which illustrates the shape of the growth at an infinitely large  $B$ . Only the principal protuberances are present in this case; regions with a negative curvature form along the direction of minimum  $B$  and  $\sigma$  when the crystal reaches a certain size.

An increase in the supercooling has a similar effect on the morphology of the protuberances. With  $\Delta T = 2 \text{ K}$ , and with the same degree of anisotropy of  $B$  and  $\sigma$  as in Fig. 3, the additional protuberances corresponding to the minimum  $\sigma$  and  $B$  do not arise.

These results agree with experimental data on the formation of the secondary protuberances (see the discussion above). In particular, they demonstrate that there are no additional protuberances as the supercooling is increased. It can be seen from Figs. 4 and 5 that comparatively small changes in the values of the factors  $Z_1$  and  $Z_2$ —measures of the anisotropy of the coefficients  $B$  and  $\sigma$ —can have a strong

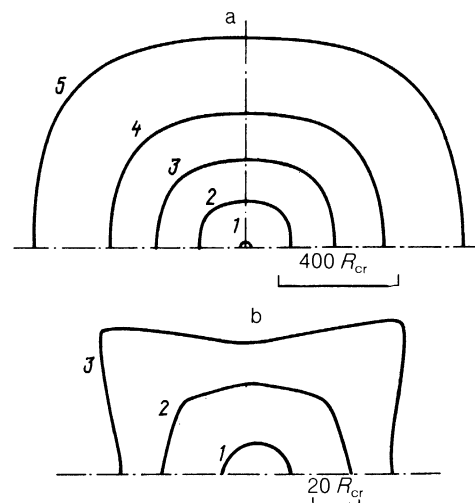


FIG. 5. Successive profiles of crystals in the case of a pronounced anisotropy in the growth velocity with  $\Delta T = 0.2 \text{ K}$ . a— $Z_1 = 0.05$ ,  $Z_2 = 0.15$ ; b— $Z_1 = 0.03$ ,  $Z_2 = 0.15$ .

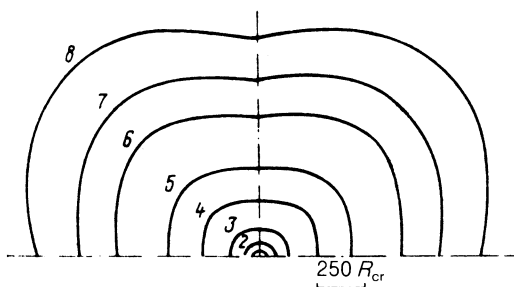


FIG. 6. Successive profiles of crystals during growth limited by heat removal ( $B = \infty$ ,  $\Delta T = 0.2$  K,  $Z_1 = 0.03$ ).  $t = 0.046, 0.46, 2.34, 10, 26, 67, 108, 174$  s.

effect on the growth velocity of the primary and secondary protuberances. Consequently, the second component, which has different effects on the anisotropy of the surface energy and the growth velocity, can cause pronounced changes in the morphology of the crystals.

A different dependence of  $\sigma$  on crystallographic direction was utilized in Ref. 12 to study the shaping of crystals on the basis of the Laplace equation. The results of the simulation in Ref. 12, like those of Refs. 6 and 11, fail to explain the features of the shaping of organic crystals described above.

The good agreement with experiment found in the present study results from the solution of the heat-conduction equation by a method which is in principle exact. It uses no assumptions other than the validity of replacing differentials by finite differences. The growth of a small particle with an initial size smaller than the diffusion radius is definitely not a steady-state process, since the surface temperature and surface concentration vary comparatively rapidly with increasing crystal size at the transition from the kinetic growth regime to the diffusion regime. The diffusion radius  $R_d$  is usually smaller than the relative-stability radius  $R_s$  for any harmonic of a periodic perturbation of the shape.

Because of the change in the roles of the surface and bulk transport processes with increasing crystal size, the effect of the anisotropy of the kinetic coefficient decreases (at an infinite value of the ratio  $BR/\alpha$ , the anisotropy of the kinetic coefficient  $B$  has no effect on the growth pattern). Protuberances which appear initially do not grow rapidly, and the crystal becomes more rounded. Above the size corresponding to the relative-stability radius, conditions favor a more rapid growth of the protuberances. In the case of the growth of succinonitrile crystals, four primary protuberances develop first. When  $R_s$  is exceeded, additional protuberances appear for the harmonic of the distortion with index 8. The essential agreement of the sizes at which the secondary protuberances appear and the values of  $R_s$  in (8) is evidence that the simulation is highly reliable.

No secondary protuberances appear if the four primary protuberances have grown to the extent that they strongly influence the entire temperature field near the crystal, and heat removal from the lagging regions is hindered. A situation of this sort develops with increasing anisotropy of the kinetic coefficient. An increase in the general supercooling of the melt has a corresponding effect. Because of the change in the relation between, on the one hand, the stability radii (which become smaller than the unit in which they are expressed,  $R_{cr}$ ) and, on the other, the diffusion radius, surface processes become more important. The anisotropy of their

kinetic coefficient thus also becomes more important.

The experiments discussed above also point to the significant role of the anisotropy of  $B$ . In the case of succinonitrile (with a small anisotropy), for example, secondary protuberances appear despite the large kinetic coefficient, while for cyclohexanol (with a large anisotropy) there are no such protuberances even at the smallest values of the supercooling attainable experimentally.

The anisotropy of the surface energy has an important effect on the angular distribution of the growth velocity at small crystal sizes. With increasing crystal size, the Gibbs-Thomson correction to the equilibrium temperature becomes less important. Anisotropy of the surface tension, however, has a very strong effect on the shape of the protuberances and on their curvature. The secondary protuberances which grow in the direction of minimum surface energy can have a curvature much larger than that of the primary protuberances. This result agrees with the experimental data. The large curvature of the secondary protuberances leads to good heat removal from them, so under certain conditions these additional protuberances may grow more rapidly than the primary ones.

## CONCLUSION

1. It has been established experimentally that when the rounded shape of a crystal becomes unstable protuberances form along certain crystallographic directions, specifically,  $\langle 100 \rangle$  directions for fcc crystals and  $\langle 100 \rangle$  and  $\langle 111 \rangle$  directions for bcc crystals. Distortion of the rounded shape in the  $\langle 100 \rangle$  direction preceding the formation of the protuberances is observed in the stage of growth in the kinetic regime (i.e., at crystal sizes at which the growth is governed by surface processes alone).

2. This numerical simulation of the growth of a rounded crystal has shown that the formation of secondary protuberances (along with the  $\langle 100 \rangle$  primary protuberances) may be governed by the degree of anisotropy of  $B$  and  $\sigma$ . It is unrelated to a change in the dependence of these properties on the crystallographic direction. The appearance or suppression of the additional protuberances results from small changes in the degree of anisotropy of  $B$  and  $\sigma$ . Furthermore, this appearance or suppression is sensitive to the magnitude of  $B$  and to the initial supercooling of the melt.

- <sup>1</sup> L. D. Landau, *Collected Papers*, Vol. 2, Pergamon, Oxford, 1965.
- <sup>2</sup> A. A. Chernov, *Modern Crystallography*, Nauka, Moscow, 1980, p. 7.
- <sup>3</sup> K. A. Jackson, in *Problems of Crystal Growth*, Mir, Moscow, 1968, p. 13.
- <sup>4</sup> D. E. Ovsienko and G. A. Alifintsev, *Metals: Electrons and Lattices*, Naukova Dumka, Kiev, 1975, p. 144.
- <sup>5</sup> G. A. Alifintsev and A. V. Mokhort, *Kristallografiya* **16**, 1054 (1971) [*Sov. Phys. Crystallogr.* **16**, 928 (1971)].
- <sup>6</sup> D. A. Kessler, J. Koplik, and H. Levine, *Phys. Rev. A* **30**, 2820 (1984).
- <sup>7</sup> A. M. Ovrutskii, *Izv. Akad. Nauk SSSR, Met. No. 4*, 80 (1980).
- <sup>8</sup> A. G. Borisov, V. V. Maslov, and O. P. Fedorov, *Metallofizika* **9**, 48 (1987).
- <sup>9</sup> G. A. Alifintsev and O. P. Fedorov, *Metallofizika* **3**, 114 (1981).
- <sup>10</sup> S. Coriell and R. Parker, in *Problems of Crystal Growth* (Russ. transl., Mir, Moscow, 1968, p. 146).
- <sup>11</sup> Y. Saito, G. Goldbek, and H. Müller-Krumbhaar, *Phys. Rev. Lett.* **58**, 547 (1987).
- <sup>12</sup> L. N. Brush and R. F. Sekerka, *J. Cryst. Growth* **96**, 419 (1989).
- <sup>13</sup> R. Wilcox, *J. Cryst. Growth* **37**, 229 (1977).
- <sup>14</sup> A. M. Ovrutskii, *Kristallografiya* **24**, 1033 (1979) [*Sov. Phys. Crystallogr.* **24**, 591 (1979)].
- <sup>15</sup> C. Herring, *Structure and Properties of Solid Surface*, Chicago, 1953, p. 5.

Translated by D. Parsons